

A flavin-based extracellular electron transfer mechanism in diverse Gram-positive bacteria

Samuel H. Light¹, Lin Su^{2,3}, Rafael Rivera-Lugo¹, Jose A. Cornejo², Alexander Louie¹, Anthony T. Iavarone⁴, Caroline M. Ajo-Franklin² & Daniel A. Portnoy^{1,5*}

Extracellular electron transfer (EET) describes microbial bioelectrochemical processes in which electrons are transferred from the cytosol to the exterior of the cell¹. Mineral-respiring bacteria use elaborate haem-based electron transfer mechanisms^{2–4} but the existence and mechanistic basis of other EETs remain largely unknown. Here we show that the food-borne pathogen *Listeria monocytogenes* uses a distinctive flavin-based EET mechanism to deliver electrons to iron or an electrode. By performing a forward genetic screen to identify *L. monocytogenes* mutants with diminished extracellular ferric iron reductase activity, we identified an eight-gene locus that is responsible for EET. This locus encodes a specialized NADH dehydrogenase that segregates EET from aerobic respiration by channelling electrons to a discrete membrane-localized quinone pool. Other proteins facilitate the assembly of an abundant extracellular flavoprotein that, in conjunction with free-molecule flavin shuttles, mediates electron transfer to extracellular acceptors. This system thus establishes a simple electron conduit that is compatible with the single-membrane structure of the Gram-positive cell. Activation of EET supports growth on non-fermentable carbon sources, and an EET mutant exhibited a competitive defect within the mouse gastrointestinal tract. Orthologues of the genes responsible for EET are present in hundreds of species across the Firmicutes phylum, including multiple pathogens and commensal members of the intestinal microbiota, and correlate with EET activity in assayed strains. These findings suggest a greater prevalence of EET-based growth capabilities and establish a previously underappreciated relevance for electrogenic bacteria across diverse environments, including host-associated microbial communities and infectious disease.

L. monocytogenes is a fermentative Gram-positive bacterium that is frequently associated with decaying plant matter in the environment, but which transforms into an intracellular pathogen on encountering a mammalian host⁵. Despite lacking a lifecycle or genes conventionally associated with EET, a 25-year-old observation that *L. monocytogenes* possessed extracellular ferric iron reductase activity⁶ led us to wonder whether a novel EET strategy existed. Because electrons transferred out of the cell can be captured by an electrode, electrochemical measurements provide a useful tool for assaying EET⁷. By performing chronoamperometry experiments, we observed that *L. monocytogenes* produces a robust electric current in the presence of growth substrate (Fig. 1a, Extended Data Fig. 1a). In addition, we found that cyclic voltammetry experiments—which monitor electric current while the electrochemical potential is systematically varied—revealed a distinctive catalytic wave reminiscent of other electrochemically active bacteria^{8,9} (Extended Data Fig. 1b). These results thus provide strong evidence that *L. monocytogenes* possesses EET activity.

To address the genetic basis of EET activity, approximately 50,000 colonies of a pooled *L. monocytogenes* *himar1* transposon library were grown on Fe³⁺-containing agar plates. Mutants with decreased

colorimetric change following an Fe²⁺-indicator overlay were visually identified and the location of their transposon insertion was mapped to the genome (Fig. 1b). From this screen, thirty-four independent transposon insertions that localized to a largely uncharacterized 8.5-kilobase locus were identified—with at least one insertion disrupting each of the eight genes in this region (Fig. 1c). Genes in the locus were assigned names on the basis of putative functions of their protein products (see ‘Gene name assignment’ in Methods for a more detailed explanation). The only transposon insertions outside the identified locus disrupt *ribU*, the substrate-binding subunit of a riboflavin transporter¹⁰

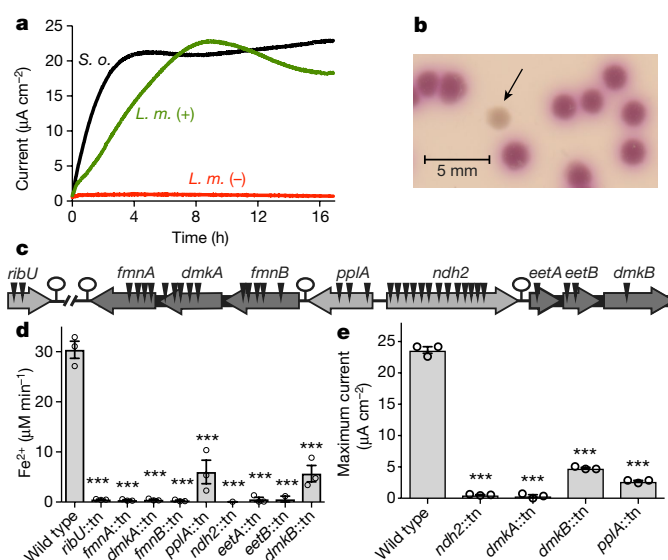


Fig. 1 | An uncharacterized genetic locus associated with EET activity. **a**, Chronoamperometry results from *L. monocytogenes* (*L. m.*)- or *Shewanella oneidensis* (*S. o.*)-inoculated electrochemical reactors. For *L. monocytogenes* experiments, an electron donor (glucose) was present in (+) or absent from (–) the medium; lactate was used as an electron donor for *S. oneidensis*. Results are representative of three independent experiments. **b**, Image of one of the thirty-six independent mutants identified from the ferric iron reduction screen, minutes after ferrozine agar overlay (arrow). **c**, Location of transposon insertions (triangles) in mutants identified as having decreased ferric iron reductase activity in the genetic screen. Arrows represent genes, with the darker grey signifying inclusion in a multi-gene operon. Previously uncharacterized genes on the locus have been assigned names based on the putative functions of the proteins they encode. **d**, Ferric iron reductase activity of transposon mutants identified from the screen. Results are expressed as mean \pm s.e.m. from three independent experiments. **e**, Maximum electric current achieved from chronoamperometry experiments with representative EET mutants. Strains that statistically differ from the wild-type strain are indicated; *** $P < 0.001$, ANOVA with Dunnett’s post-test.

¹Department of Molecular and Cell Biology, University of California, Berkeley, Berkeley, CA, USA. ²Molecular Foundry, Molecular Biophysics and Integrated Bioimaging, and Synthetic Biology Institute, Lawrence Berkeley National Laboratory, Berkeley, CA, USA. ³State Key Laboratory of Bioelectronics, School of Biological Science and Medical Engineering, Southeast University, Nanjing, 210018, China. ⁴QB3/Chemistry Mass Spectrometry Facility, University of California, Berkeley, Berkeley, CA, USA. ⁵Plant and Microbial Biology, University of California, Berkeley, Berkeley, CA, USA. *e-mail: portnoy@berkeley.edu

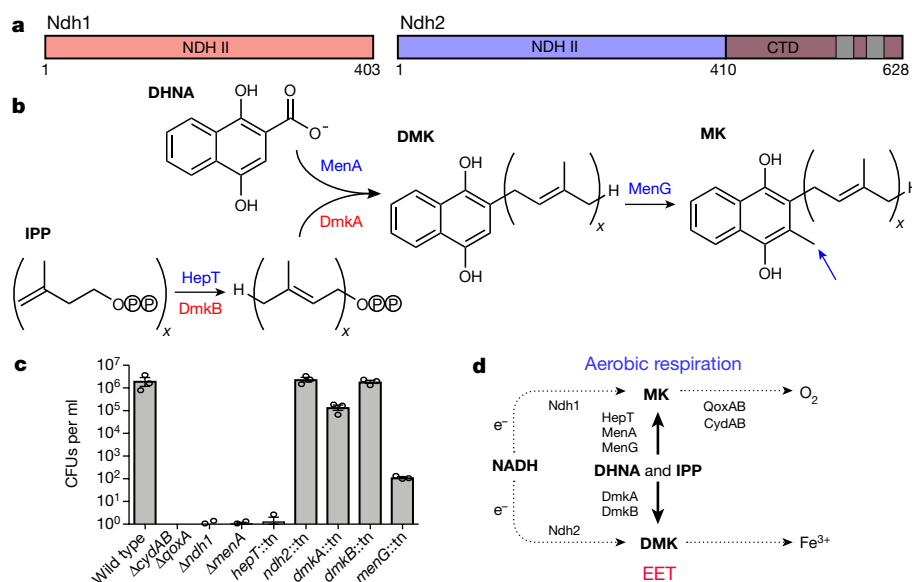


Fig. 2 | A parallel electron transfer pathway segregates EET from aerobic respiration. **a**, Domain layout of the *L. monocytogenes* proteins Ndh1 and Ndh2. CTD, C-terminal domain; NDH II, type II NADH dehydrogenase domain. Grey regions represent predicted transmembrane helices. **b**, Predicted reactions catalysed by *L. monocytogenes* DmkA and DmkB, the paralogous proteins MenA and HepT, and MenG (highlighted by blue arrow). DHNA, 1,4-dihydroxy-2-naphthoyl-CoA; DMK, demethylmenaquinone; IPP, isopentenyl pyrophosphate; MK, menaquinone; *x*, an unknown number of isoprene repeats (which may

differ between the two quinones). **c**, Colony-forming units (CFUs) after 24 h in aerobic respiration medium. Results from three independent experiments are expressed as mean \pm s.e.m. The Δ cydAB Δ qoxA mutant lacks terminal cytochrome oxidases and thus provides an aerobic-respiration-deficient control. **d**, Probable electron transfer pathways inferred from mutants with EET (red) or aerobic respiration (blue) phenotypes. Dashed arrows highlight the path of electron flow and solid lines track quinone synthesis.

(Fig. 1c). We confirmed that the mutants had diminished ferric iron reductase (Fig. 1d) and electrochemical activity (Fig. 1e, Extended Data Fig. 1b) and then turned to study the molecular basis of EET.

Type II NADH dehydrogenase—or Ndh1 in *L. monocytogenes*—catalyses electron exchange from cytosolic NADH to a lipid-soluble quinone derivative, which is the first step in the respiratory electron transport chain¹¹. Ndh2, which is encoded by one of the genes in the EET locus, is a protein with an N-terminal type II NADH dehydrogenase domain and a unique transmembrane C-terminal domain that is absent from functionally characterized enzymes (Fig. 2a). Consistent with Ndh2 being a novel NADH dehydrogenase, we observed that EET activation correlated with cellular NAD⁺ levels (Extended Data Fig. 2). Furthermore, the proteins DmkA and DmkB—which are encoded by two other genes in the EET locus—are paralogues of the highly conserved microbial enzymes MenA and HepT, which catalyse terminal steps in the production of the quinone demethylmenaquinone (Fig. 2b). In *Escherichia coli*, three different quinones—demethylmenaquinone, menaquinone and ubiquinone—are used to selectively channel electrons to different electron acceptors¹². By analogy, we reasoned that a distinct quinone derivative and NADH dehydrogenase might functionally segregate electron fluxes for EET and aerobic respiration.

To clarify the relationship between EET and aerobic respiration, we formulated an ‘aerobic respiration medium’ that contained non-fermentable glycerol as the sole carbon source. Despite exhibiting wild-type levels of ferric iron reductase activity (Extended Data Fig. 3a), Δ cydAB Δ qoxA (a positive control that lacks terminal cytochrome oxidases), Δ menA, *hepT::tn* and Δ ndh1 strains failed to grow on aerobic respiration medium (Fig. 2c). By contrast, EET mutants grew similarly to wild-type strains under these conditions (Fig. 2c). Moreover, *menG*—which encodes the enzyme that converts demethylmenaquinone to menaquinone—is contained on an operon with *hepT* and is essential for growth on aerobic respiration medium, but not ferric iron reductase activity (Fig. 2c, Extended Data Fig. 3). Collectively, these results support the conclusion that a demethylmenaquinone derivative used by Ndh2 and a menaquinone derivative used by Ndh1 are selective for downstream enzymes that function in EET and aerobic respiration, respectively (Fig. 2d).

We next sought to address the downstream steps responsible for electron transfer from the quinone pool to extracellular electron acceptors. FmnB is a predicted lipoprotein that is annotated as possessing FMN transferase activity. Homologous FMN transferases catalyse a post-translational modification in which an FMN moiety is covalently linked to a threonine side chain of substrate proteins^{13,14} (Fig. 3a). To identify protein substrates of FmnB, wild-type and *fmnB::tn* cells were subjected to a comparative mass spectrometric analysis. Only two *L. monocytogenes* peptides met the criteria of selective FMNylation in the wild-type sample and both of these mapped to distinct regions in the protein product of the neighbouring gene in the EET locus, PplA (Supplementary Table 1).

Similar to FmnB, PplA is a predicted lipoprotein and, consistent with this prediction, a trypsin-shaving experimental approach, in which extracellular-surface-associated proteins liberated through a partial digestion of the cell wall are identified by mass spectrometry, confirmed that PplA is associated with the surface of the cell (Supplementary Table 2). The N-terminal lipidation site on PplA is followed by approximately 30 amino acids that are predicted to be unstructured. N-terminal unstructured regions are a common feature of bacterial lipoproteins and are thought to provide a loose tether that allows the active portion of the protein to diffuse further from the membrane and to partially or fully penetrate the cell wall¹⁵. This property, coupled with the covalently bound redox-active FMNs, is consistent with PplA representing the extracellular component of the EET machinery that facilitates electron transfer—via its FMNs—to extracellular electron acceptors.

Following its unstructured N-terminal region, PplA has sequential domains that share 59% sequence identity with each other. From the proteomic analysis, it is evident that the FMNylated threonines on PplA assume equivalent positions on each of these related domains (Fig. 3b). To further clarify the mechanism of FMNylation, we tested FmnB substrate specificity using recombinant FmnB and PplA. These assays confirm that FmnB catalyses FMNylation of PplA and demonstrate that the enzyme specifically uses flavin adenine dinucleotide (FAD) as a substrate (Fig. 3c, Extended Data Fig. 4).

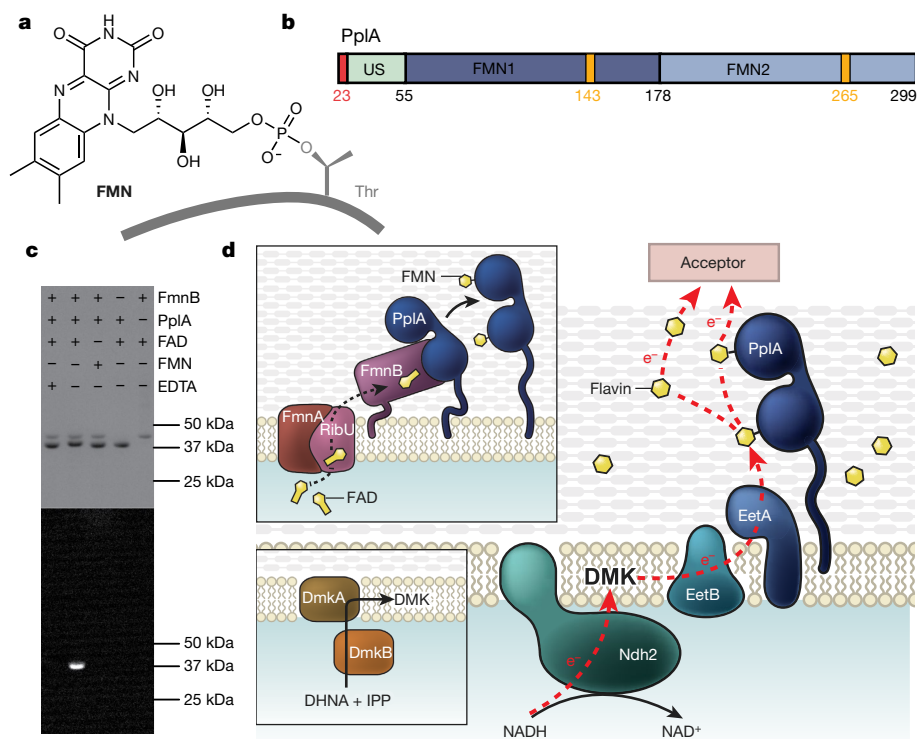


Fig. 3 | A surface-associated flavoprotein establishes the extracellular component of the EET apparatus. **a**, Post-translational modification catalysed by the FMN transferase family of enzymes, of which FmnB is a member^{13,14}. **b**, Domain architecture of PplA. FMN1, FMNylated domain 1; FMN2, FMNylated domain 2; US, unstructured. The lipitated cysteine on the N terminus after signal peptidase processing is shown in red and FMNylated threonines are shown in yellow. **c**, Analysis of FmnB substrate specificity. SDS-PAGE of recombinant PplA after incubation under specified conditions. Ultraviolet illumination of the gel (bottom) enables visualization of protein with covalently bound flavin. Results are

Because both FmnB and PplA are membrane-anchored lipoproteins, a source of FAD substrate is required for FmnB to FMNylate PplA on the surface of the cell. The only transposon insertions identified outside the EET locus disrupt *ribU*, which has previously been shown to encode the substrate-binding subunit of an energy-coupling factor (ECF) transporter that functions in riboflavin uptake¹⁰. In addition to a substrate-binding subunit, ECF transporters contain a transmembrane subunit and two distinct ATPase subunits, which drive the transport of substrate across the membrane¹⁰ (Extended Data Fig. 5a). FmnA in the EET locus shares 50% sequence identity with the transmembrane subunit of the RibU-ECF riboflavin transporter (EcfT) and this led us to propose that FmnA interacted with RibU to promote FAD secretion (Extended Data Fig. 5b). Consistent with this interpretation, proteomic analysis of *ribU::tn* and *fmnA::tn* strains revealed a marked decrease in PplA FMNylation (Supplementary Table 1). Furthermore, addition of FAD to the growth medium specifically restored ferric iron reductase activity to the *ribU::tn* and *fmnA::tn* strains (Extended Data Fig. 5c). On the basis of these findings, we propose that RibU and FmnA establish a transporter that secretes the FAD required for FmnB-catalysed FMNylation of PplA.

The term ‘extracellular electron shuttle’ refers to redox-active small molecules that are cyclically reduced by cells and oxidized by extracellular electron acceptors^{16,17}. The relevance of shuttles for EET is exemplified by *Shewanella* species, which use an efflux-type transporter to secrete flavins that shuttle electrons to acceptors that are not directly contacting the cell^{18–20}. In contrast to *Shewanella*, *L. monocytogenes* is a flavin auxotroph and thus by definition environmental flavins must be present in its replicative niche. Indeed, micromolar flavin concentrations are typical of nutrient-rich environments, such as the plant biomass and mammalian hosts in which

representative of three independent experiments. See Supplementary Fig. 1 for uncropped gel. **d**, Model of the molecular basis of EET. DmkA and DmkB synthesize a demethylmenaquinone derivative (bottom inset). RibU and FmnA secrete FAD that is used by FmnB to post-translationally modify PplA (top inset). EET is achieved by a series of electron transfers. Ndh2 transfers electrons from NAD to DMK. Electrons are transferred from DMK to FMN groups on PplA or free flavin shuttles—possibly with involvement from uncharacterized membrane proteins in the EET locus, EetA and EetB—and ultimately to a terminal electron acceptor.

L. monocytogenes proliferates^{21,22}. To determine whether flavins could be used as electron shuttles, we tested the effect of exogenous riboflavin, FMN and FAD on EET activity. Injection of FMN into an *L. monocytogenes*-inoculated electrochemical chamber resulted in a pronounced increase in electric current (Extended Data Fig. 6a). Moreover, while cells immersed in soluble ferric iron exhibited a high baseline level of reductase activity that was unresponsive to flavins, flavins caused a marked concentration-dependent enhancement in the reduction of insoluble ferric (hydr)oxide (Extended Data Fig. 6b). These data thus support the conclusion that *L. monocytogenes* can use environmental flavins to shuttle electrons to outlying acceptors.

Integrating all of our insights into the roles of the components of the EET apparatus, we propose a molecular model of electron travel from intracellular NADH to membrane-confined quinone, then to extracellular flavoprotein (and/or other shuttles), and ultimately to a kinetically favourable terminal electron acceptor (Fig. 3d). To determine whether EET established a bona fide growth-supporting activity, we next screened a library of common microbial growth substrates and found that the inclusion of ferric iron or an electrode was required for anaerobic growth on the sugar alcohols xylitol and D-arabitol (Fig. 4a, Extended Data Fig. 7). Genes for aerobic respiration but not EET were essential for aerobic growth on xylitol, whereas this pattern was reversed under anaerobic conditions—that is, EET genes were essential and aerobic respiration genes dispensable (Fig. 4a, Extended Data Fig. 7). These data demonstrate that the distinct electron transport chains that segregate aerobic respiration and EET promote aerobic and anaerobic growth, respectively.

We next asked whether EET has a role in host colonization. Consistent with EET being dispensable for aerobic growth,

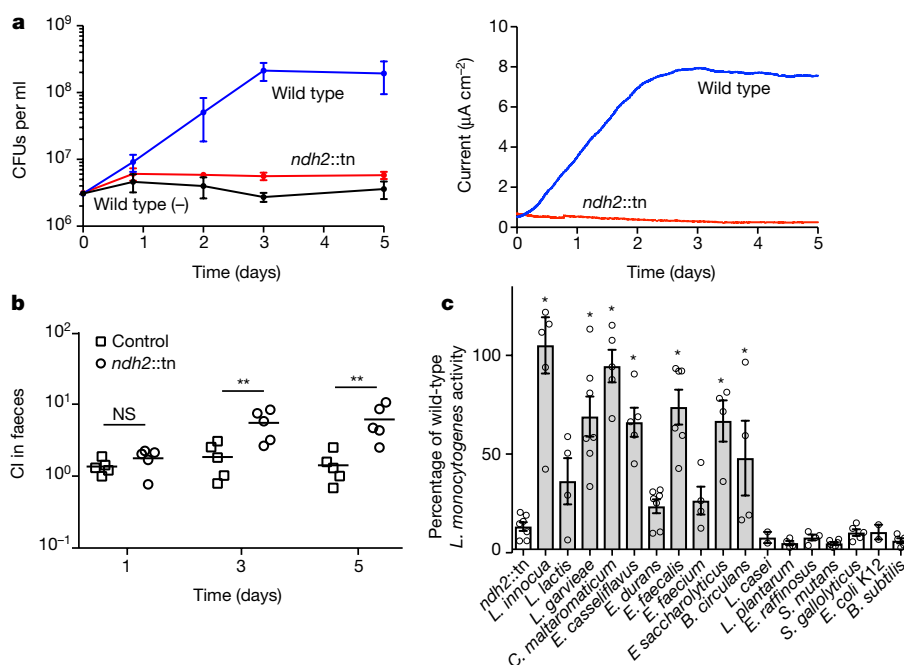


Fig. 4 | EET supports anaerobic growth, confers a competitive advantage in the intestinal lumen, and is active in multiple Firmicutes.

a, *L. monocytogenes* CFUs (left) and electric current (right) from chronoamperometry experiments conducted with xylitol growth medium. (–), control condition without an electrode. Results from three independent experiments are expressed as mean \pm s.e.m. **b**, Mice ($n = 5$) were fed bread inoculated with a 1:1 mixture of Δhly and $\Delta hly ndh2::tn$ *L. monocytogenes* strains. The competitive index (CI) at three time points after infection is indicated. Median values and statistically significant differences compared to a control that competed two Δhly strains are indicated; $**P = 0.01$, unpaired two-sided *t*-test. Results are representative of three independent experiments. **c**, Iron reductase activity in a panel of Firmicutes species, expressed as a percentage of wild-type *L. monocytogenes* activity. Results from at least three independent experiments ($n = 7$ for *ndh2::tn*, *Lactococcus garvieae* and *Enterococcus*

durans; $n = 6$ for *Listeria innocua*, *E. faecalis* and *Streptococcus mutans*; $n = 5$ for *Carnobacterium maltaromaticum*, *Enterococcus casseliflavus*, *Streptococcus gallolyticus* and *Bacillus subtilis*; $n = 4$ for *Lactococcus lactis*, *Enterococcus faecium*, *Enterococcus saccharolyticus*, *Bacillus circulans*, *Lactobacillus plantarum* and *Enterococcus raffinosus*; $n = 3$ for *Lactobacillus casei* and *E. coli* K12) are expressed as mean \pm s.e.m. Strains that statistically differ from *ndh2::tn* are indicated; $*P < 0.05$, ANOVA with Dunnett's post-test. Some members of Lactobacillales lack the ability to synthesize DHNA, the precursor for demethylmenaquinone biosynthesis, and require an exogenous source for quinone-dependent processes³⁶. Organisms with genes in the EET locus and *menC* (which catalyses an essential step in DHNA biosynthesis) are coloured grey. *L. casei*, *L. plantarum* and *E. raffinosus* contain genes for EET, but not *menC*. The remaining species lack genes in the EET locus.

EET-deficient mutants resembled wild-type *L. monocytogenes* in an intracellular macrophage growth assay and an intravenous infection model (Extended Data Fig. 8). Because anaerobic growth mechanisms are important for microbial proliferation within the intestinal lumen^{23,24}, we proposed that the food-borne pathogen might use EET in this context. Consistent with the hypothesis, the faecal burden of the *ndh2::tn* strain was decreased approximately sixfold in a streptomycin-pretreated model of *L. monocytogenes* intestinal colonization (Fig. 4b). These results thus suggest a role for EET within the dysbiotic gut and raise the possibility that EET constitutes a generally important metabolic activity within the mammalian gastrointestinal tract.

We next turned to the phylogenetic distribution of the genes responsible for EET. BLAST searches revealed that homologues of these genes are widespread in hundreds of species that span the Firmicutes phylum (Extended Data Fig. 9a, Supplementary Table 3). Many of these genes are likely to encode functional EET systems, as the identified locus is typically conserved, though noteworthy distinctions are evident in some genomes (Extended Data Fig. 9b). Microorganisms that possess a locus with EET genes adopt a wide range of different lifestyles, including within thermophilic (*Caldanaerobius* spp., *Thermoanaerobacter* spp. and so on) and halophilic (*Halolactibacillus* spp., *Halothermothrix* spp. and so on) habitats. Orthologues of the identified genes in the EET locus are found in a number of human pathogens (*Clostridium perfringens*, *Enterococcus faecalis*, *Streptococcus dysgalactiae* and so on), members of the human microbiota (*Clostridium* spp., *Enterococcus* spp., *Streptococcus* spp. and so on) and lactic acid bacteria that have

commercial applications in food fermentation or probiotics (*Lactococcus* spp., *Lactobacillus* spp., *Oenococcus* spp., *Tetragenococcus* spp. and so on) (Supplementary Table 3). The functionality of identified loci could explain previous reports of EET-like activity in a number of species^{25–35} and assays of ferric iron reductase activity of a panel of Firmicutes provided additional evidence that the presence of necessary genetic components correlates with EET activity (Fig. 4c).

In conclusion, our study reveals a novel electron transport chain that supports growth on extracellular electron acceptors. This mechanism lacks an elaborate multi-haem apparatus and, partly by taking advantage of the single-membrane architecture of the Gram-positive cell, is characterized by considerably fewer electron transfer steps than comparable systems in mineral-respiring Gram-negative bacteria¹. The genes identified in the EET locus are present in a wide-ranging group of microorganisms that occupy a diverse array of ecological niches. Defying conventional views of EET, this distinctive system is abundant in bacteria that prioritize fermentative metabolic strategies and reside in nutrient-rich environments, including the lactic acid bacteria. Within this context, environmental flavins may represent a feature of the ecological landscape that can be exploited to promote EET activity. These observations suggest that, rather than being a specialized process confined to mineral-respiring bacteria, the use of extracellular electron acceptors represents a fundamental facet of microbial metabolism that is relevant across diverse environments. In addition to obvious bioenergetic applications, the characterization of a flavin-based EET mechanism thus establishes further avenues for the study of electrochemical activities throughout the microbial world.

Online content

Any methods, additional references, Nature Research reporting summaries, source data, statements of data availability and associated accession codes are available at <https://doi.org/10.1038/s41586-018-0498-z>.

Received: 2 January 2018; Accepted: 3 August 2018;

Published online 12 September 2018.

- Shi, L. et al. Extracellular electron transfer mechanisms between microorganisms and minerals. *Nat. Rev. Microbiol.* **14**, 651–662 (2016).
- Myers, C. R. & Nealson, K. H. Bacterial manganese reduction and growth with manganese oxide as the sole electron acceptor. *Science* **240**, 1319–1321 (1988).
- Lovley, D. R. & Phillips, E. J. Novel mode of microbial energy metabolism: organic carbon oxidation coupled to dissimilatory reduction of iron or manganese. *Appl. Environ. Microbiol.* **54**, 1472–1480 (1988).
- Carlson, H. K. et al. Surface multiheme c-type cytochromes from *Thermincola potens* and implications for respiratory metal reduction by Gram-positive bacteria. *Proc. Natl Acad. Sci. USA* **109**, 1702–1707 (2012).
- Freitag, N. E., Port, G. C. & Miner, M. D. *Listeria monocytogenes* – from saprophyte to intracellular pathogen. *Nat. Rev. Microbiol.* **7**, 623–628 (2009).
- Deneer, H. G. & Boychuk, I. Reduction of ferric iron by *Listeria monocytogenes* and other species of *Listeria*. *Can. J. Microbiol.* **39**, 480–485 (1993).
- Kim, B. H., Kim, H. J., Hyun, M. S. & Park, D. H. Direct electrode reaction of Fe(III)-reducing bacterium, *Shewanella putrefaciens*. *J. Microbiol. Biotechnol.* **9**, 127–131 (1999).
- Marsili, E., Rollefson, J. B., Baron, D. B., Hozalski, R. M. & Bond, D. R. Microbial biofilm voltammetry: direct electrochemical characterization of catalytic electrode-attached biofilms. *Appl. Environ. Microbiol.* **74**, 7329–7337 (2008).
- Xu, S. J. Y. & El-Naggar, M. Y. Disentangling the roles of free and cytochrome-bound flavins in extracellular electron transport from *Shewanella oneidensis* MR-1. *Electrochim. Acta* **198**, 49–55 (2016).
- Karpowich, N. K., Song, J. M., Cocco, N. & Wang, D. N. ATP binding drives substrate capture in an ECF transporter by a release-and-catch mechanism. *Nat. Struct. Mol. Biol.* **22**, 565–571 (2015).
- Kerscher, S., Dröse, S., Zickermann, V. & Brandt, U. The three families of respiratory NADH dehydrogenases. *Results Probl. Cell Differ.* **45**, 185–222 (2008).
- Uden, G. & Bongaerts, J. Alternative respiratory pathways of *Escherichia coli*: energetics and transcriptional regulation in response to electron acceptors. *Biochim. Biophys. Acta* **1320**, 217–234 (1997).
- Bertsova, Y. V. et al. Alternative pyrimidine biosynthesis protein ApbE is a flavin transferase catalyzing covalent attachment of FMN to a threonine residue in bacterial flavoproteins. *J. Biol. Chem.* **288**, 14276–14286 (2013).
- Deka, R. K., Brautigam, C. A., Liu, W. Z., Tomchick, D. R. & Norgard, M. V. Evidence for posttranslational protein flavinylation in the syphilis spirochete *Treponema pallidum*: structural and biochemical insights from the catalytic core of a periplasmic flavin-trafficking protein. *MBio* **6**, e00519-15 (2015).
- Zückert, W. R. Secretion of bacterial lipoproteins: through the cytoplasmic membrane, the periplasm and beyond. *Biochim. Biophys. Acta* **1843**, 1509–1516 (2014).
- Glasser, N. R., Saunders, S. H. & Newman, D. K. The colorful world of extracellular electron shuttles. *Annu. Rev. Microbiol.* **71**, 731–751 (2017).
- Brutinel, E. D. & Gralnick, J. A. Shuttling happens: soluble flavin mediators of extracellular electron transfer in *Shewanella*. *Appl. Microbiol. Biotechnol.* **93**, 41–48 (2012).
- Marsili, E. et al. *Shewanella* secretes flavins that mediate extracellular electron transfer. *Proc. Natl Acad. Sci. USA* **105**, 3968–3973 (2008).
- von Canstein, H., Ogawa, J., Shimizu, S. & Lloyd, J. R. Secretion of flavins by *Shewanella* species and their role in extracellular electron transfer. *Appl. Environ. Microbiol.* **74**, 615–623 (2008).
- Kotloski, N. J. & Gralnick, J. A. Flavin electron shuttles dominate extracellular electron transfer by *Shewanella oneidensis*. *MBio* **4**, e00553-12 (2013).
- Powers, H. J. Riboflavin (vitamin B-2) and health. *Am. J. Clin. Nutr.* **77**, 1352–1360 (2003).
- Hühner, J., Ingles-Prieto, Á., Neusüß, C., Lämmerhofer, M. & Janovjak, H. Quantification of riboflavin, flavin mononucleotide, and flavin adenine dinucleotide in mammalian model cells by CE with LED-induced fluorescence detection. *Electrophoresis* **36**, 518–525 (2015).
- Winter, S. E. et al. Gut inflammation provides a respiratory electron acceptor for *Salmonella*. *Nature* **467**, 426–429 (2010).
- Winter, S. E. et al. Host-derived nitrate boosts growth of *E. coli* in the inflamed gut. *Science* **339**, 708–711 (2013).
- Slobodkin, A. I. et al. Dissimilatory reduction of Fe(III) by thermophilic bacteria and archaea in deep subsurface petroleum reservoirs of western Siberia. *Curr. Microbiol.* **39**, 99–102 (1999).
- Roh, Y. et al. Isolation and characterization of metal-reducing thermoanaerobacter strains from deep subsurface environments of the Piceance Basin, Colorado. *Appl. Environ. Microbiol.* **68**, 6013–6020 (2002).
- Ogg, C. D. & Patel, B. K. *Fervidicola ferrireducens* gen. nov., sp. nov., a thermophilic anaerobic bacterium from geothermal waters of the Great Artesian Basin, Australia. *Int. J. Syst. Evol. Microbiol.* **59**, 1100–1107 (2009).
- Ogg, C. D. & Patel, B. K. *Thermotalea metallivorans* gen. nov., sp. nov., a thermophilic, anaerobic bacterium from the Great Artesian Basin of Australia. *Int. J. Syst. Evol. Microbiol.* **59**, 964–971 (2009).
- Ogg, C. D., Greene, A. C. & Patel, B. K. *Thermovenabulum gondwanense* sp. nov., a thermophilic anaerobic Fe(III)-reducing bacterium isolated from microbial mats thriving in a Great Artesian Basin bore runoff channel. *Int. J. Syst. Evol. Microbiol.* **60**, 1079–1084 (2010).
- Ogg, C. D. & Patel, B. K. *Fervidicella metallireducens* gen. nov., sp. nov., a thermophilic, anaerobic bacterium from geothermal waters. *Int. J. Syst. Evol. Microbiol.* **60**, 1394–1400 (2010).
- Masuda, M., Freguia, S., Wang, Y. F., Tsujimura, S. & Kano, K. Flavins contained in yeast extract are exploited for anodic electron transfer by *Lactococcus lactis*. *Bioelectrochemistry* **78**, 173–175 (2010).
- Zhang, E., Cai, Y., Luo, Y. & Piao, Z. Riboflavin-shuttled extracellular electron transfer from *Enterococcus faecalis* to electrodes in microbial fuel cells. *Can. J. Microbiol.* **60**, 753–759 (2014).
- Dong, Y. et al. *Orenia metallireducens* sp. nov. strain Z6, a novel metal-reducing member of the phylum Firmicutes from the deep subsurface. *Appl. Environ. Microbiol.* **82**, 6440–6453 (2016).
- Keogh, D. et al. Extracellular electron transfer powers *Enterococcus faecalis* biofilm metabolism. *MBio* **9**, e00626-17 (2018).
- Pankratova, G., Leech, D., Gorton, L. & Hederstedt, L. Extracellular electron transfer by the Gram-positive bacterium *Enterococcus faecalis*. *Biochemistry* **57**, 4597–4603 (2018).
- Pedersen, M. B., Gaudu, P., Lechardeur, D., Petit, M. A. & Gruss, A. Aerobic respiration metabolism in lactic acid bacteria and uses in biotechnology. *Annu. Rev. Food Sci. Technol.* **3**, 37–58 (2012).

Acknowledgements We thank G. Chen, J.-D. Sauer, E. Stevens, M. Marco and N. Freitag for providing bacterial strains; H. Carlson, A. Williamson and J. Coates for helpful feedback; and N. Garellis for experimental assistance. Research reported in this publication was supported by funding from the National Institute of Allergy and Infectious Diseases of the National Institutes of Health (F32AI136389 to S.H.L., 1P01 AI063302 to D.A.P., and 1R01 AI27655 to D.A.P.), the Office of Naval Research (N0001417WX01603 to C.M.A.-F.), and the China Scholarship Council (no. 201606090098 to L.S.). A mass spectrometer used in this study was purchased with NIH support (grant 1S10OD020062-01). Work at the Molecular Foundry was supported by the Office of Science, Office of Basic Energy Sciences, of the US Department of Energy under Contract No. DE-AC02-05CH11231.

Reviewer information *Nature* thanks N. Freitag, J. Gralnick, K. Nealson and G. Reguera for their contribution to the peer review of this work.

Author contributions S.H.L., A.T.I., C.M.A.-F. and D.A.P. designed the study. S.H.L., L.S. and J.A.C. performed electrochemical experiments. S.H.L. and A.T.I. performed mass spectrometric experiments. S.H.L., A.L. and R.R.-L. performed microbiological and biochemical experiments. S.H.L. and D.A.P. wrote the manuscript.

Competing interests D.A.P. has a consulting relationship with and a financial interest in Aduro Biotech; both he and the company stand to benefit from the commercialization of this research.

Additional information

Extended data is available for this paper at <https://doi.org/10.1038/s41586-018-0498-z>.

Supplementary information is available for this paper at <https://doi.org/10.1038/s41586-018-0498-z>.

Reprints and permissions information is available at <http://www.nature.com/reprints>.

Correspondence and requests for materials should be addressed to D.A.P. **Publisher's note:** Springer Nature remains neutral with regard to jurisdictional claims in published maps and institutional affiliations.

METHODS

***L. monocytogenes* strains and growth conditions.** All *L. monocytogenes* strains used in this study were derived from wild-type 10403S (Supplementary Table 4). Transduction methods were used to introduce transposons into distinct genetic backgrounds, as previously described^{37,38}. *L. monocytogenes* cells were grown at 37 °C and spectrophotometrically measured by optical density at a wavelength of 600 nm (OD₆₀₀). Anaerobic conditions were achieved with the BD GasPak EZ pouch system or an anaerobic chamber (Coy Laboratory Products) with an environment of 2% H₂ balanced in N₂.

Filter-sterilized brain–heart infusion medium (Difco) or variants of chemically defined *Listeria* synthetic medium (LSM)³⁹ were used in all studies. Aerobic respiration medium replaced the glucose in LSM with 50 mM glycerol. The requirement of an electron acceptor to support *L. monocytogenes* growth on xylitol was identified by comparing aerobic versus anaerobic (absent an alternative electron acceptor) growth on carbon sources, using PM1 and PM2A plates of the Phenotype MicroArray (Biolog). ‘Xylitol medium’ replaced the glucose in LSM with 50 mM xylitol.

Gene name assignment. The identified EET locus is widely conserved in *L. monocytogenes* isolates and encompasses the genes *lmg_02179–lmg_02186* in *L. monocytogenes* 10403S (which correspond to *lmo2634–lmo2641* in *L. monocytogenes* EGD-e). Identified genes in the EET locus were assigned *dmk* or *fmn* prefixes based on putative roles in demethylmenaquinone biosynthesis or PplA FMNylation, respectively. The *et* prefix was assigned to the remaining genes, which at present lack high-confidence functional assignments. The only previously named gene, *pplA*, was so-called on the basis of the role of its cleaved signal peptide as a signalling pheromone⁴⁰ (a function that seems to be unrelated to the mature protein).

Bioelectrochemical characterization and measurements. Chronoamperometry and cyclic voltammetry were carried out using a Bio-Logic Science Instruments potentiostat model VSP-300. All measurements were performed using double chamber electrochemical cells (Extended Data Fig. 1a) and consisted of an Ag/AgCl reference electrode (CH Instruments), a Pt wire counter electrode (Alfa Aesar), and a 6.35-mm-thick graphite felt working electrode with a 16-mm radius (Alfa Aesar).

Electrochemical cells were prepared with 120 ml of modified LSM (containing 0.8 μM FMN as the sole flavin) and an open circuit potential was performed in the absence of bacteria. Once the current stabilized, the electrochemical cell was inoculated to a final OD₆₀₀ of ~0.1. The medium in the electrochemical chamber was mixed with a magnetic stir bar for the course of the experiment. For current acquisition, the applied potential was set at +0.4 V versus Ag/AgCl. To maintain anaerobic conditions, electrochemical cells were continuously purged with N₂ gas. Cyclic voltammetry measurements in the potential region of –0.8 to +0.4 V versus Ag/AgCl and a scan rate of 10 mV s⁻¹ were conducted immediately before inoculation and 3 h later. Electric currents are reported as a function of the geometric surface area of the electrode. To test the effect of flavins on electrochemical activity, FMN was injected into the *L. monocytogenes*-inoculated electrochemical chamber to a final concentration of 1 μM.

For *S. oneidensis* experiments, the glucose in LSM was replaced with sodium lactate and *S. oneidensis* was inoculated to an OD₆₀₀ of 0.1. Growth-supporting *L. monocytogenes* experiments on xylitol medium were conducted in a similar fashion, but the electrochemical cell was inoculated to an OD₆₀₀ of ~0.002 and the medium from the electrochemical chamber was sampled at regular intervals for the enumeration of CFUs.

Screen of mutants with diminished ferric iron reductase activity. A previously described method was adapted to screen for *L. monocytogenes* mutants with diminished ferric iron reductase activity⁶. Approximately 250 CFUs per plate of a pooled *himar1* transposon library, generated as previously described³⁸, were grown on brain–heart infusion agar supplemented with 0.1 mg/ml ferric ammonium citrate. After 24 h at 37 °C, plates were removed from the incubator and a 10-ml overlay (0.8% agarose and 2 mM ferrozine) was applied. Colorimetric change resulting from ferrozine binding to Fe²⁺ was visually tracked for ~10 min. Colonies with diminished colorimetric change were selected and the location of the transposon insertion identified by Sanger sequencing, as previously described⁴¹.

Ferrozine assay of ferric iron reductase activity. *L. monocytogenes* cells grown to mid-log phase were washed twice, normalized to an OD₆₀₀ of 0.5, and resuspended in fresh medium supplemented with 4 mM ferrozine. Experiments were initiated by adding 100 μl of cells to an equivalent volume of 50 mM ferric ammonium citrate or ferric (hydr)oxide and were conducted in triplicate at 37 °C in 96-well format using a plate reader. OD₅₆₂ measurements were made every 30 s for up to an hour. Maximal rates (typically over 2 min) calculated from a Fe²⁺ standard curve are reported. Assays were generally performed in LSM, with glucose serving as the electron donor. However, because some of the respiratory mutants grew poorly in these conditions, these strains were assayed in brain–heart infusion medium (with glucose remaining as the electron donor). For FAD complementation studies, before washing steps, strains grown to mid-log were split and—after adding

0.5 mM FAD to one aliquot—incubated for 1 h at 37 °C. To test the effect of flavins, riboflavin, FMN or FAD was titrated into cells resuspended in a LSM base that lacked flavins.

To prepare other species (detailed in Supplementary Table 4) for the ferric iron reductase assay, cells were grown anaerobically in brain–heart infusion medium for 36 h. Sub-cultures in brain–heart infusion medium supplemented with 25 mM ferric ammonium citrate were then grown to mid-log phase. Cells were washed twice, resuspended in fresh brain–heart infusion medium and cell densities were normalized to wild-type *L. monocytogenes*. Next, ferrozine was added to a final concentration of 2 mM and 100 μl of cells were dispensed in a 96-well plate. The experiment was initiated by adding 100 μl of brain–heart infusion medium supplemented with 10 mM ferric ammonium citrate and OD₅₆₂ measurements were made as described for the *L. monocytogenes* ferric iron reductase assay.

***L. monocytogenes* growth on xylitol and ferric iron.** To test electron acceptor usage capabilities, xylitol medium was inoculated with *L. monocytogenes* and incubated at 25 °C in an anaerobic chamber. Conditions testing putative electron acceptors contained 50 mM ferric ammonium citrate or ferric (hydr)oxide, prepared as previously described⁴². For the ferric ammonium citrate experiments, 50 mM sodium citrate was included in the control condition that lacked ferric ammonium citrate and CFUs were enumerated following overnight incubation in a 96-well plate (Greiner Bio-One). Ferric (hydr)oxide experiments were conducted in a 6-well plate (Costar) and CFUs were enumerated 6 days after inoculation.

NAD⁺ and NADH measurements. *L. monocytogenes* cells grown overnight in LSM were washed and resuspended in 500 μl of medium. Cells were then split and 50 mM ferric ammonium citrate was added to one aliquot. To test aerobic conditions, 14-ml tubes were placed in a shaking (200 r.p.m.) incubator. To achieve microaerophilic conditions, the headspace in the tube was purged with argon gas and the tightly capped tube was placed in a stationary incubator. After 1.5 h at 37 °C, bacteria were collected by centrifugation, resuspended in PBS and lysed by vortexing with 0.1-mm-diameter zirconia–silica beads. NAD⁺ and NADH measurements were performed using the NAD/NADH-Glo Assay (Promega).

Assay of FmnB FMN transferase activity. Constructs of *fmnB* and *pplA* that truncated the signal peptide were subcloned into the pMCSG58 vector. Protein overexpression and purification followed previously described protocols⁴³. Purified PplA and FmnB were incubated overnight at a 10:1 molar ratio in assay buffer (0.5 M NaCl and 10 mM Tris, pH 8.3) with putative flavin substrates. Because homologous FMN transferases require a magnesium cofactor¹³, the effect of the chelator EDTA on activity was tested. Samples were analysed by SDS–PAGE and protein bands with covalent flavin modifications were visualized by UV illumination.

To identify the basis of post-translational modifications, intact protein mass measurements of PplA were made using a Synapt G2-Si mass spectrometer that was equipped with an electrospray ionization source and a C₄ protein ionKey (inner diameter: 150 μm, length: 50 mm, particle size: 1.7 μm), and connected in-line with an Acquity M-class ultra-performance liquid chromatography system (UPLC; Waters). Acetonitrile, formic acid (Fisher Optima grade, 99.9%) and water purified to a resistivity of 18.2 MΩ-cm (at 25 °C) using a Milli-Q Gradient ultrapure water purification system (Millipore) were used to prepare mobile phase solvents. Solvent A was 99.9% water/0.1% formic acid and solvent B was 99.9% acetonitrile/0.1% formic acid (v/v). The elution program consisted of a linear gradient from 1% to 10% B (v/v) over 1 min, a linear gradient from 10% to 90% B over 4 min, isocratic flow at 90% B for 5 min, a linear gradient from 90% to 1% B over 2 min, and isocratic flow at 1% B for 18 min, at a flow rate of 2 μl/min. The ionKey column and the autosampler compartment were maintained at 40 °C and 6 °C, respectively. Mass spectra were acquired in the positive ion mode and continuum format, operating the time-of-flight analyser in resolution mode, with a scan time of 0.5 s, over the range *m/z* = 400 to 5,000. Mass spectral deconvolution was performed using ProMass software (version 2.5 SR-1, Novatia).

***L. monocytogenes* protein trypsinization.** One millilitre of *L. monocytogenes* cells grown in LSM to mid-log phase was washed, resuspended in 100 μl of 100 mM NH₄HCO₃ (pH 7.5), and incubated at 100 °C for 10 min. Cells were lysed by bead beating for 15 min at 4 °C. RapiGest SF (Waters) was added to lysed cells at a final concentration of 0.1% and the sample was incubated at 100 °C for 5 min. After adding 5 μl of 100 mM dithiothreitol, samples were incubated at 58 °C for 30 min. Next, 15 μl of 100 mM iodoacetamide was added and samples were incubated for an additional 30 min. Samples were then digested overnight with 10 μl Trypsin Gold (Promega). The following morning, 10 μl of 5% trifluoroacetic acid was added and samples were incubated at 37 °C for 90 min. Samples were centrifuged for 30 min to remove hydrolysed RapiGest, and supernatant was collected.

***L. monocytogenes* intracellular growth assays.** Bone-marrow-derived macrophages prepared from 6- to 8-week-old female mice were plated overnight on coverslips and infected with *L. monocytogenes* strains at a multiplicity of infection of 0.1. Macrophage monolayers were washed with PBS and fresh medium was added thirty minutes after infection. At 1 h post-infection, 50 μg/ml gentamicin was added to kill extracellular bacteria. To enumerate *L. monocytogenes* CFUs,

macrophages were lysed by transferring coverslips to 10 ml of water, as previously described⁴⁴.

***L. monocytogenes* intravenous infections.** Eight-week-old female C57BL/6 mice (The Jackson Laboratory) were infected with 1×10^5 CFUs in 200 μ l of PBS by tail vein injection. Forty-eight hours post-infection, spleens and livers were collected, homogenized and plated for the enumeration of CFUs.

***L. monocytogenes* oral infections.** Previously described models of *L. monocytogenes* oral infection were adapted to address the role of EET in the intestinal lumen^{45,46}. Prior to infection, 5 mg/ml of streptomycin sulfate was added to the drinking water of 8-week-old female C57BL/6 mice (The Jackson Laboratory). After 24 h, mice were transferred to fresh cages and chow was removed to initiate an overnight fast. Forty-eight hours after streptomycin addition to the water, mice were isolated, fed a small piece of bread with 3 μ l of butter and an inoculum with 10^8 CFUs of *L. monocytogenes*, and returned to cages containing standard drinking water and chow. To confine *L. monocytogenes* to the intestinal lumen, a Δ *hly* parental strain (which has greatly reduced intracellular growth and spread) was used in these experiments. Inoculums were prepared with a 1:1 ratio of Δ *hly* and an erythromycin-resistant Δ *hly* strain (Δ *hly erm*^R, derived as previously described⁴⁷) or Δ *hly* and Δ *hly ndh2::tn*. Following infection, stools were collected, homogenized and dilutions were plated. Because total parental strain CFUs did not statistically differ between conditions, results are simply reported as a competitive index (that is, the ratio of streptomycin to erythromycin-resistant CFUs). These studies were carried out in strict accordance with the recommendations in the Guide for the Care and Use of Laboratory Animals of the National Institutes of Health. All protocols were reviewed and approved by the Animal Care and Use Committee at the University of California, Berkeley (AUP-2016-05-8811).

Identification of protein substrates of FmnB. Wild-type and *fmnB::tn* strains grown in LSM were prepared for proteomic analysis as described in '*L. monocytogenes* protein trypsinization'. Peptides with >50% FMNylated peptide relative ion abundance in the wild-type sample and <5% in the *fmnB::tn* sample were identified using Progenesis QI for Proteomics software (version 4.0, Waters) and validated by manual inspection of the data. To address the FMNylation status of PplA, *ribU::tn* and *fmnA::tn* mutants were prepared in the same manner.

Trypsin-shaving analysis of surface-associated proteins. Trypsin-shaving experiments were adapted from a previously described method⁴. Cells grown in brain-heart infusion medium were washed twice and resuspended in a shaving buffer (1 M sucrose + 1 mM HEPES, pH 7). Lysozyme from chicken egg white (Sigma) was added to a concentration of 0.1 mg/ml. Cells were incubated at 37 °C for 60 min and released surface-associated components were separated from the cell by centrifugation. The supernatant (surface-associated protein fraction) was dialysed overnight in digestion buffer (100 mM NH₄HCO₃, pH 7.5) and the pellet (total protein fraction) was resuspended in digestion buffer. Samples were prepared for proteomic experiments as described in '*L. monocytogenes* protein trypsinization'. A label-free relative quantification approach^{48,49} implemented in Progenesis QI for Proteomics software (version 4.0, Waters) identified proteins that were disproportionately abundant in the surface-associated fraction.

Liquid chromatography-mass spectrometry analysis of trypsin-digested proteins. Samples of trypsin-digested proteins were analysed in triplicate using the Acquity M-class UPLC and Synapt G2-Si mass spectrometer, as follows. The mass spectrometer was equipped with a nano-electrospray ionization source that was connected in-line with the UPLC. The UPLC was equipped with trapping (Symmetry C18, inner diameter: 180 μ m, length: 20 mm, particle size: 5 μ m) and analytical (HSS T3, inner diameter: 75 μ m, length: 250 mm, particle size: 1.8 μ m, Waters) columns. Solvent A was 99.9% water/0.1% formic acid and solvent B was 99.9% acetonitrile/0.1% formic acid (v/v). The elution program consisted of a linear gradient from 1% to 10% B (v/v) over 2 min, a linear gradient from 10% to 35% B over 90 min, a linear gradient from 35% to 90% B over 1 min, isocratic flow at 90% B for 6 min, a linear gradient from 90% to 1% B over 1 min, and isocratic flow at 1% B for 20 min, at a flow rate of 300 nl/min. The column and autosampler compartments were maintained at 35 °C and 6 °C, respectively. Ion mobility-enabled HD-MS^E data^{50,51} were acquired in the positive ion mode and continuum format, operating the time-of-flight analyser in resolution mode, with a scan time of 0.5 s, over the range *m/z* = 50 to 2,000. An optimized wave velocity of 850 m/s was used for the travelling wave ion mobility cell. Collision-induced dissociation was performed in the ion transfer cell with a collision-energy ramp from 30 to 78 V.

Data acquisition was controlled using MassLynx software (version 4.1), and tryptic peptides were identified using Progenesis QI for Proteomics software (version 4.0, Waters).

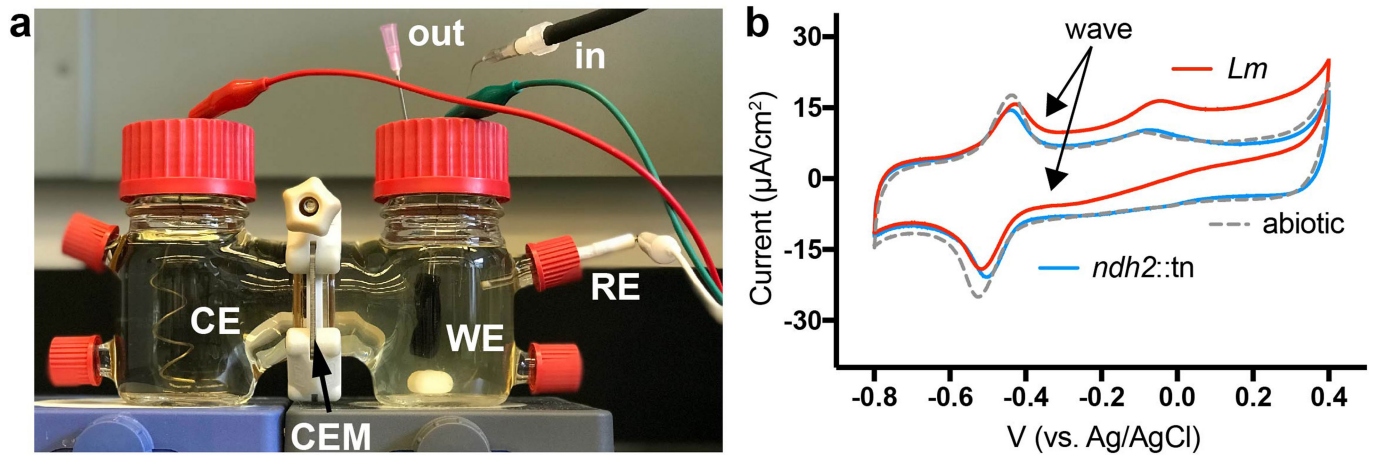
Bioinformatics analysis of identified genes in the EET locus. Ndh2 homologues were identified by searching the sequence of the unique C-terminal domain of Ndh2 on the PSI-BLAST server⁵². To perform a phylogenetic analysis, representative homologues were selected and aligned by ClustalW⁵³. The maximum likelihood method was used to infer the evolutionary history of identified sequences in Mega 7.0.26 and confidence limits of branch points were estimated by 1,000 bootstrap replications^{54,55}. The information about EET genetic loci summarized in Supplementary Table 3 was acquired by analysing genomic context of identified genes in the PATRIC 3.5.1 database (<https://www.patricbrc.org>).

Statistics and reproducibility. No statistical methods were used to predetermine sample size. The experiments were not randomized and investigators were not blinded to allocation during experiments and outcome assessment. Statistical analyses were performed in Prism 5 for Mac OS X (GraphPad Software) and Progenesis QI for Proteomics version 4.0.

Reporting summary. Further information on research design is available in the Nature Research Reporting Summary linked to this paper.

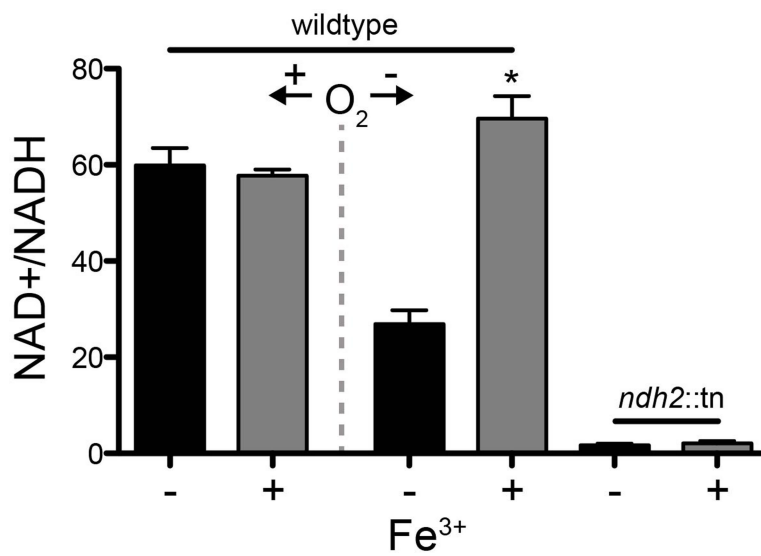
Data availability. The datasets generated during the current study are available from the corresponding author on reasonable request.

37. Hodgson, D. A. Generalized transduction of serotype 1/2 and serotype 4b strains of *Listeria monocytogenes*. *Mol. Microbiol.* **35**, 312–323 (2000).
38. Zemansky, J. et al. Development of a mariner-based transposon and identification of *Listeria monocytogenes* determinants, including the peptidyl-prolyl isomerase PrsA2, that contribute to its hemolytic phenotype. *J. Bacteriol.* **191**, 3950–3964 (2009).
39. Whiteley, A. T., Pollock, A. J. & Portnoy, D. A. The PAMP c-di-AMP is essential for *Listeria monocytogenes* growth in rich but not minimal media due to a toxic increase in (p)ppGpp. *Cell Host Microbe* **17**, 788–798 (2015).
40. Xayarath, B., Alonzo, F. III & Freitag, N. E. Identification of a peptide-pheromone that enhances *Listeria monocytogenes* escape from host cell vacuoles. *PLoS Pathog.* **11**, e1004707 (2015).
41. Burke, T. P. et al. *Listeria monocytogenes* is resistant to lysozyme through the regulation, not the acquisition, of cell wall-modifying enzymes. *J. Bacteriol.* **196**, 3756–3767 (2014).
42. Lovley, D. R. & Phillips, E. J. Organic matter mineralization with reduction of ferric iron in anaerobic sediments. *Appl. Environ. Microbiol.* **51**, 683–689 (1986).
43. Light, S. H., Cahoon, L. A., Halavaty, A. S., Freitag, N. E. & Anderson, W. F. Structure to function of an α -glucan metabolic pathway that promotes *Listeria monocytogenes* pathogenesis. *Nat. Microbiol.* **2**, 16202 (2016).
44. Portnoy, D. A., Jacks, P. S. & Hinrichs, D. J. Role of hemolysin for the intracellular growth of *Listeria monocytogenes*. *J. Exp. Med.* **167**, 1459–1471 (1988).
45. Bou Ghanem, E. N. et al. InA promotes dissemination of *Listeria monocytogenes* to the mesenteric lymph nodes during food borne infection of mice. *PLoS Pathog.* **8**, e1003015 (2012).
46. Becattini, S. et al. Commensal microbes provide first line defense against *Listeria monocytogenes* infection. *J. Exp. Med.* **214**, 1973–1989 (2017).
47. Auerbuch, V., Lenz, L. L. & Portnoy, D. A. Development of a competitive index assay to evaluate the virulence of *Listeria monocytogenes* actA mutants during primary and secondary infection of mice. *Infect. Immun.* **69**, 5953–5957 (2001).
48. Neilson, K. A. et al. Less label, more free: approaches in label-free quantitative mass spectrometry. *Proteomics* **11**, 535–553 (2011).
49. Nahnsen, S., Bielow, C., Reinert, K. & Kohlbacher, O. Tools for label-free peptide quantification. *Mol. Cell. Proteomics* **12**, 549–556 (2013).
50. Plumb, R. S. et al. UPLC/MS^E; a new approach for generating molecular fragment information for biomarker structure elucidation. *Rapid Commun. Mass Spectrom.* **20**, 1989–1994 (2006).
51. Shliaha, P. V., Bond, N. J., Gatto, L. & Lilley, K. S. Effects of traveling wave ion mobility separation on data independent acquisition in proteomics studies. *J. Proteome Res.* **12**, 2323–2339 (2013).
52. Altschul, S. F. et al. Gapped BLAST and PSI-BLAST: a new generation of protein database search programs. *Nucleic Acids Res.* **25**, 3389–3402 (1997).
53. Larkin, M. A. et al. Clustal W and Clustal X version 2.0. *Bioinformatics* **23**, 2947–2948 (2007).
54. Jones, D. T., Taylor, W. R. & Thornton, J. M. The rapid generation of mutation data matrices from protein sequences. *Comput. Appl. Biosci.* **8**, 275–282 (1992).
55. Kumar, S., Stecher, G. & Tamura, K. MEGA7: molecular evolutionary genetics analysis version 7.0 for bigger datasets. *Mol. Biol. Evol.* **33**, 1870–1874 (2016).



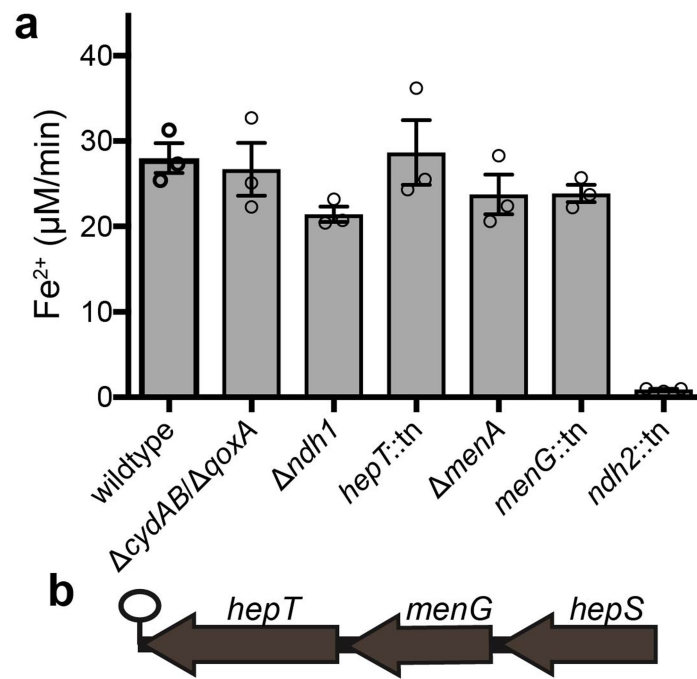
Extended Data Fig. 1 | Electrochemical analyses of *L. monocytogenes*.
a, The double chamber cell used for electrochemical experiments. CE, counter electrode; CEM, cation exchange membrane; RE, reference electrode; WE, working electrode. Inlets and outlets for N_2 gas are

labelled. **b**, Cyclic voltammograms of wild-type and *ndh2::tn* strains of *L. monocytogenes*. 'Abiotic' refers to an uninoculated control. Arrows highlight the initiation of the catalytic wave. Results are representative of three independent experiments.



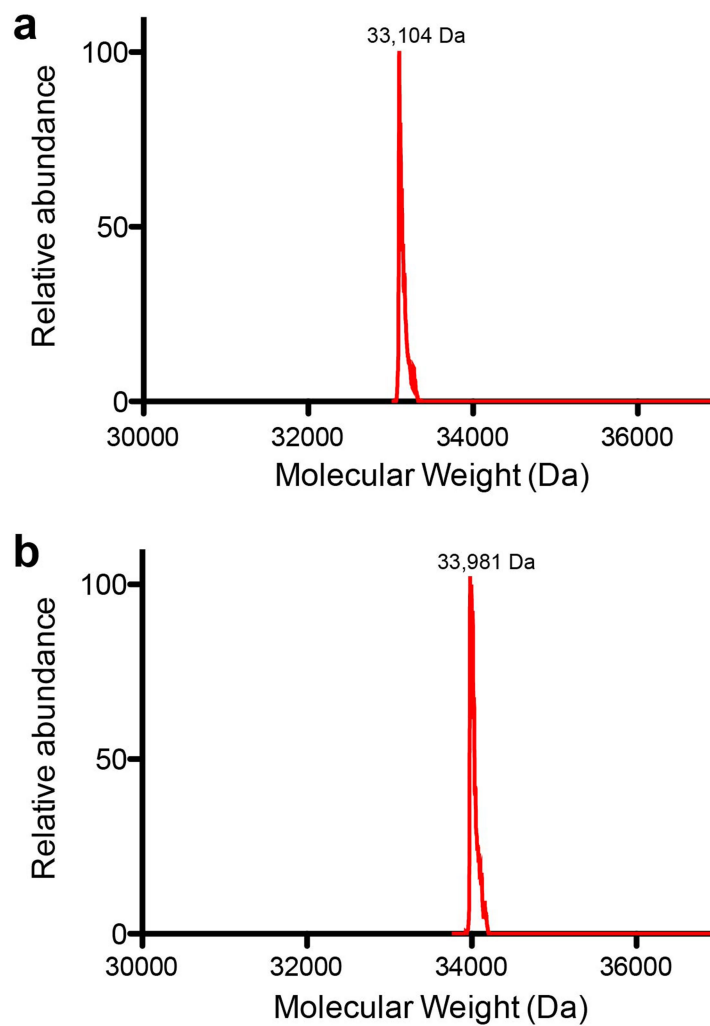
Extended Data Fig. 2 | EET activity maintains cellular redox homeostasis. Ratio of NAD⁺ to NADH in wild-type and *ndh2::tn* strains supplemented with ferric ammonium citrate under aerobic or microaerophilic conditions. Results from three independent experiments

are expressed as mean \pm s.e.m. A statistically significant difference between microaerophilic cells incubated with or without iron is indicated; * $P = 0.0015$, unpaired two-sided t -test.



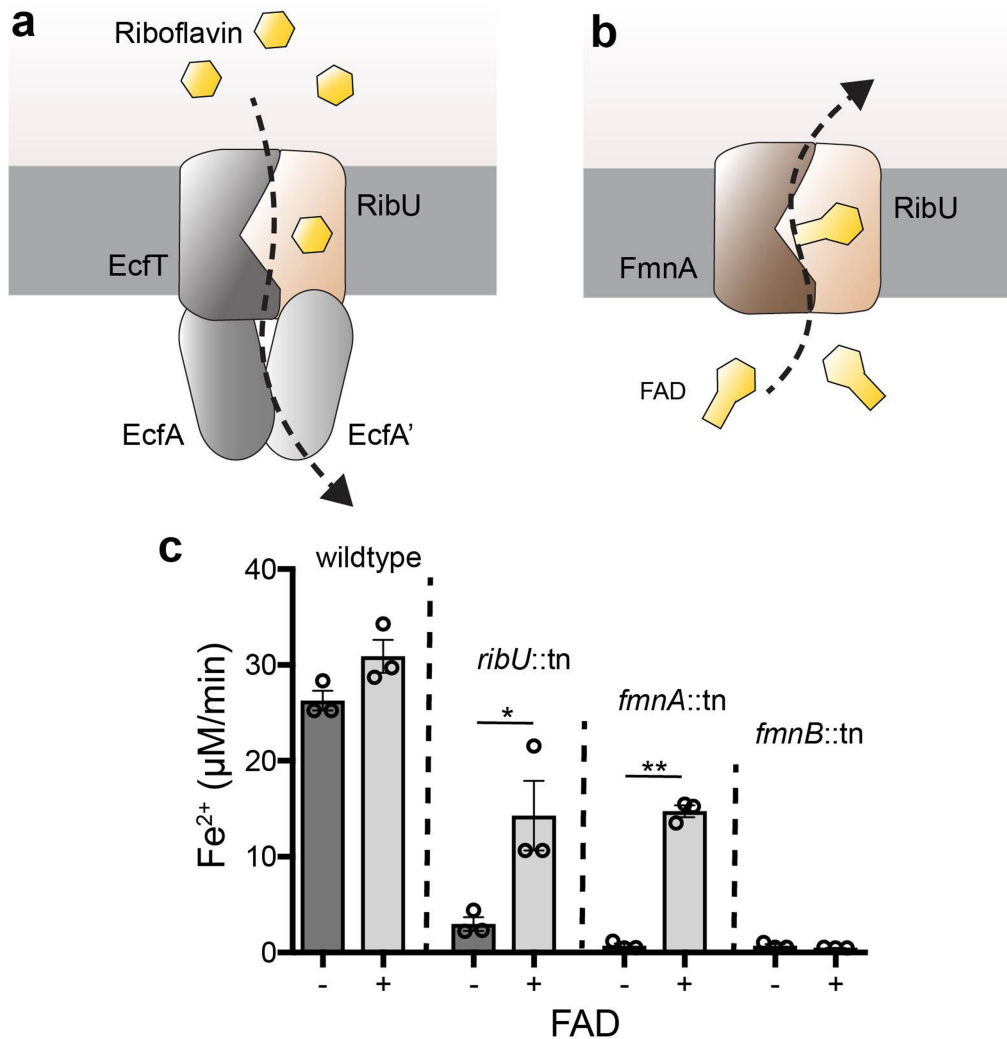
Extended Data Fig. 3 | Evidence that a distinct menaquinone derivative functions in aerobic respiration. a, Ferric iron reductase activity of mutants described in Fig. 2 demonstrates that genes essential for growth on aerobic respiration medium are dispensable for EET. Results from three independent experiments are expressed as mean

\pm s.e.m. **b,** The *L. monocytogenes* *hep* operon. Notably, *menG*—which encodes demethylmenaquinone transferase (the enzyme that converts demethylmenaquinone to menaquinone) (Fig. 2b)—neighbours the *hepT* and *hepS* genes, which function in quinone biosynthesis and are essential for aerobic respiration (Fig. 2c).



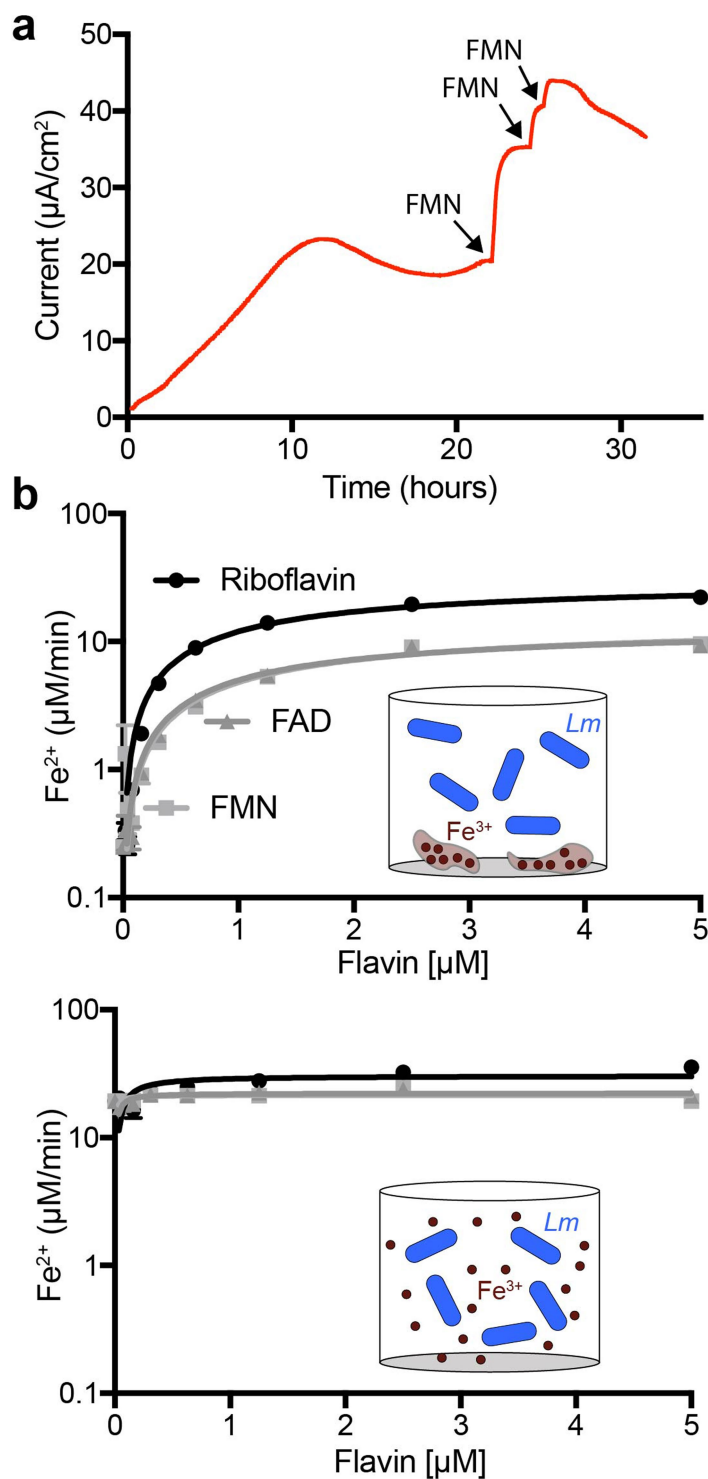
Extended Data Fig. 4 | Recombinant FmnB FMNylates PplA at two discrete sites. a, b, Deconvoluted mass spectra from a single experiment of recombinant PplA (a) and recombinant PplA incubated with

FAD + FmnB (b). The observed molecular weight change (877 Da) is consistent with two post-translational FMNylations (2×438.3 Da) on PplA.



Extended Data Fig. 5 | Proposed role of RibU and FmnA in FAD secretion. **a**, Simplified adaptation of a previously proposed model of *L. monocytogenes* riboflavin uptake through the RibU, EcfT, EcfA and EcfA' transporter¹⁰. According to this model, EcfT, EcfA and EcfA' couple ATP hydrolysis with conformational changes that result in substrate bound to RibU being released into the cytosol. **b**, On the basis of protein homology (FmnA shares 50% sequence identity with EcfT) and the expectation that extracellular FAD is required for FmnB to catalyse FMNylation of PplA, we propose that the FmnA interacts with RibU

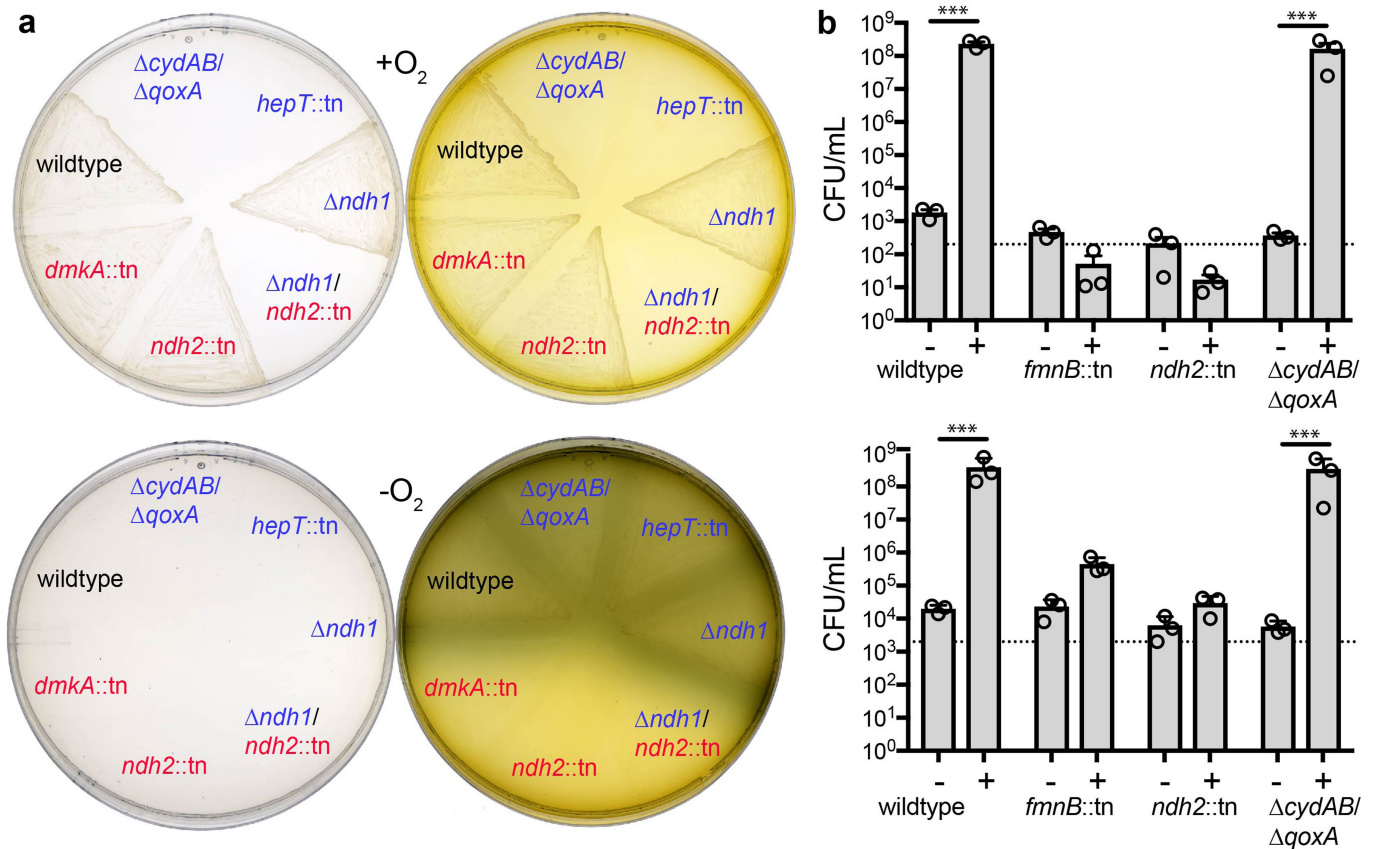
to promote FAD secretion. **c**, Ferric iron reductase activity of strains incubated with 0.5 mM FAD for 1 h. The ability of exogenous FAD to specifically rescue ferric iron reductase activity in the *fmnA::tn* and *ribU::tn* strains is consistent with FmnA and RibU functioning in FAD secretion. Results from three independent experiments are expressed as mean \pm s.e.m. Statistically significant differences between untreated and FAD-treated cells are indicated; * $P = 0.038$, ** $P < 0.0001$, unpaired two-sided *t*-test.



Extended Data Fig. 6 | Flavin shuttles promote EET activity.

a. Chronoamperometry results from *L. monocytogenes*-inoculated electrochemical reactors with $1\ \mu\text{M}$ FMN injections at the indicated time points. Results are representative of three independent experiments. **b.** The effect of flavins on *L. monocytogenes* (*Lm*) ferric iron reductase activity

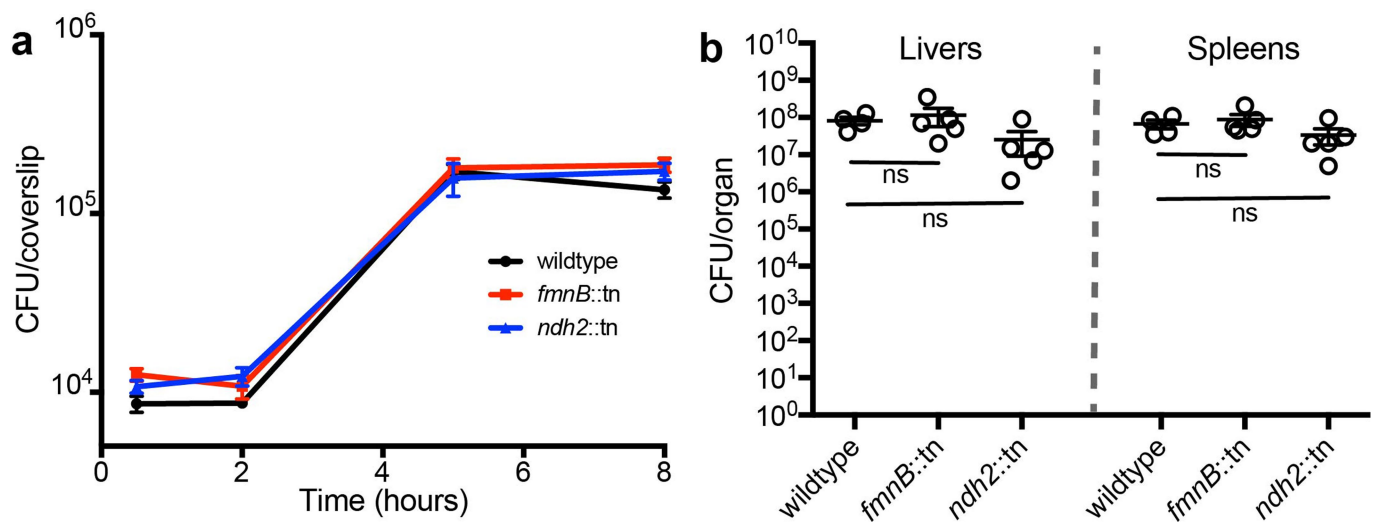
with insoluble ferric (hydr)oxide (top) and soluble ferric ammonium citrate (bottom). With insoluble substrate the local iron concentration for most cells is low, whereas with soluble substrate the concentration of iron in the direct vicinity of cells is high (insets). Results from three independent experiments are expressed as mean \pm s.e.m.



Extended Data Fig. 7 | EET supports anaerobic growth on ferric iron.

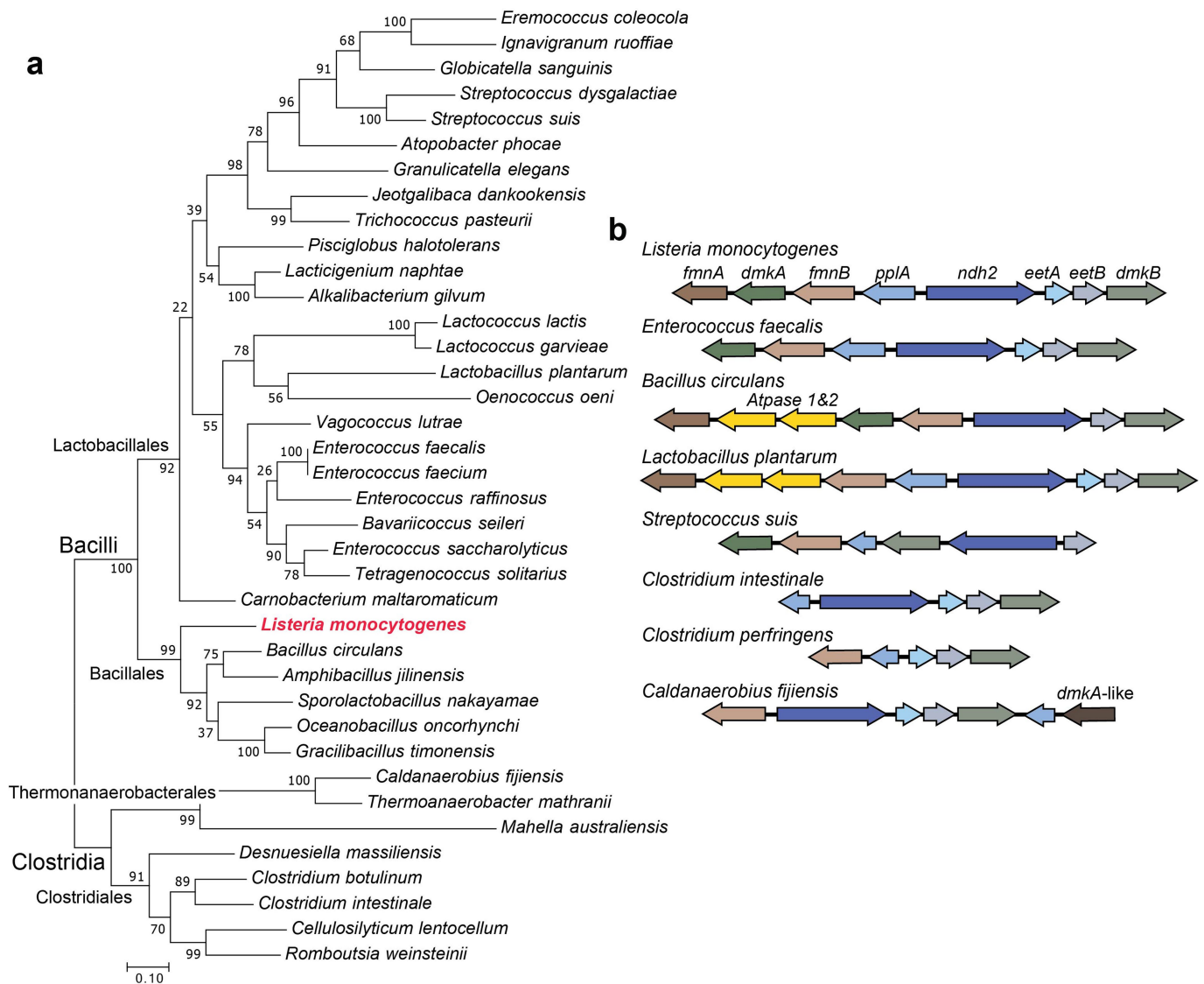
a, Growth following incubation of *L. monocytogenes* strains on xylitol medium without (left) or with (right) ferric iron under aerobic (top) or anaerobic (bottom) conditions. Results are representative of three independent experiments. Strain labels are coloured based on attributed deficiencies (Fig. 2d) in aerobic respiration (blue) or EET (red). Ndh1 and Ndh2 are probably functionally redundant under aerobic conditions, as a growth phenotype is only observed in the double mutant. Note the visual evidence of ferrous iron production in the agar adjoining anaerobically

growing cells. **b**, CFUs of *L. monocytogenes* strains anaerobically incubated in xylitol medium without (–) or with (+) ferric supplementation. Results for soluble ferric ammonium citrate (top) and insoluble ferric (hydr) oxide (bottom) are shown. Dashed lines denote the number of cells at the start of the experiment. Results from three independent experiments are expressed as mean \pm s.e.m. Statistically significant differences in the ferric iron-supplemented condition are noted; *** $P < 0.0001$, unpaired two-sided *t*-test.



Extended Data Fig. 8 | EET genes are dispensable for *L. monocytogenes* intracellular growth. **a**, Mouse bone-marrow-derived macrophages were infected with *L. monocytogenes*, and CFUs were enumerated at the indicated times. Results from three independent experiments are

expressed as mean \pm s.e.m. **b**, *L. monocytogenes* burdens in mouse organs ($n = 5$) 48 h after intravenous infection. Representative results from two independent experiments are expressed as median and s.e.



Extended Data Fig. 9 | Identified EET loci are widespread in the Firmicutes phylum. a, Phylogenetic tree constructed from select Ndh2 homologue sequences. A more comprehensive list of organisms that possess an EET locus is provided in Supplementary Table 3. Labels on the branches refer to the percentage of replicate trees that gave the depicted branch topology in a bootstrap test of 1,000 replicates. **b**, Distinct EET loci from select genomes are shown. Although the arrangement of genes varies, a locus with genes associated with EET is present in many genomes. Some loci contain ECF transporter ATPase subunits (homologous to

those depicted in Extended Data Fig. 5a) that probably function with RibU and FmnA subunits in flavin transport. The *dmkA*-like gene found in *Caldanaerobius fijiensis* (and other genomes) lacks homology to *dmkA*, but is annotated as catalysing the same reaction. The *pplA* variant in some genomes contains a single FMNylated domain (rather than two) and this property is indicated by a shorter arrow. A few bacteria (including *Lactococcus* spp.) lack a recognizable locus and distribute genes associated with EET throughout the genome.

Reporting Summary

Nature Research wishes to improve the reproducibility of the work that we publish. This form provides structure for consistency and transparency in reporting. For further information on Nature Research policies, see [Authors & Referees](#) and the [Editorial Policy Checklist](#).

Statistical parameters

When statistical analyses are reported, confirm that the following items are present in the relevant location (e.g. figure legend, table legend, main text, or Methods section).

n/a Confirmed

- The exact sample size (n) for each experimental group/condition, given as a discrete number and unit of measurement
- An indication of whether measurements were taken from distinct samples or whether the same sample was measured repeatedly
- The statistical test(s) used AND whether they are one- or two-sided
Only common tests should be described solely by name; describe more complex techniques in the Methods section.
- A description of all covariates tested
- A description of any assumptions or corrections, such as tests of normality and adjustment for multiple comparisons
- A full description of the statistics including central tendency (e.g. means) or other basic estimates (e.g. regression coefficient) AND variation (e.g. standard deviation) or associated estimates of uncertainty (e.g. confidence intervals)
- For null hypothesis testing, the test statistic (e.g. F , t , r) with confidence intervals, effect sizes, degrees of freedom and P value noted
Give P values as exact values whenever suitable.
- For Bayesian analysis, information on the choice of priors and Markov chain Monte Carlo settings
- For hierarchical and complex designs, identification of the appropriate level for tests and full reporting of outcomes
- Estimates of effect sizes (e.g. Cohen's d , Pearson's r), indicating how they were calculated
- Clearly defined error bars
State explicitly what error bars represent (e.g. SD, SE, CI)

Our web collection on [statistics for biologists](#) may be useful.

Software and code

Policy information about [availability of computer code](#)

Data collection

MassLynx software (version 4.1) was used in mass spectrometric data collection.

Data analysis

Data were analyzed for statistical significance using Prism 5 for Mac OS X. BLAST-PSI was used to identify FLEET homologs. Protein sequence alignments were performed in ClustalW and a phylogenetic tree was built using Mega 7.0.26. The PATRIC 3.5.1 database was used for analysis of the genomic context of FLEET genes. For mass spectrometric analyses, tryptic peptides were identified using Progenesis Q1 for Proteomics software (version 4.0, Waters). Mass spectral deconvolution of intact protein mass spectrometric data performed using ProMass software (version 2.5 SR-1, Novatia, Monmouth Junction, NJ).

For manuscripts utilizing custom algorithms or software that are central to the research but not yet described in published literature, software must be made available to editors/reviewers upon request. We strongly encourage code deposition in a community repository (e.g. GitHub). See the Nature Research [guidelines for submitting code & software](#) for further information.

Data

Policy information about [availability of data](#)

All manuscripts must include a [data availability statement](#). This statement should provide the following information, where applicable:

- Accession codes, unique identifiers, or web links for publicly available datasets
- A list of figures that have associated raw data
- A description of any restrictions on data availability

The datasets generated during the current study are available from the corresponding author on reasonable request.

Field-specific reporting

Please select the best fit for your research. If you are not sure, read the appropriate sections before making your selection.

Life sciences Behavioural & social sciences

For a reference copy of the document with all sections, see [nature.com/authors/policies/ReportingSummary-flat.pdf](https://www.nature.com/authors/policies/ReportingSummary-flat.pdf)

Life sciences

Study design

All studies must disclose on these points even when the disclosure is negative.

Sample size	Sample sizes were based upon accepted conventions within the field and no explicit power analysis were carried out.
Data exclusions	No data were excluded from analysis.
Replication	All experiments were independently repeated and all attempts to replicate the experiments were successful.
Randomization	Animals were randomly assigned to groups (cages) prior to experimentation.
Blinding	Investigators were not blinded to group allocation during data collection or analysis.

Materials & experimental systems

Policy information about [availability of materials](#)

n/a	Involvement in the study
<input checked="" type="checkbox"/>	<input type="checkbox"/> Unique materials
<input checked="" type="checkbox"/>	<input type="checkbox"/> Antibodies
<input checked="" type="checkbox"/>	<input type="checkbox"/> Eukaryotic cell lines
<input type="checkbox"/>	<input checked="" type="checkbox"/> Research animals
<input checked="" type="checkbox"/>	<input type="checkbox"/> Human research participants

Research animals

Policy information about [studies involving animals](#); [ARRIVE guidelines](#) recommended for reporting animal research

Animals/animal-derived materials

Method-specific reporting

n/a	Involvement in the study
<input checked="" type="checkbox"/>	<input type="checkbox"/> ChIP-seq
<input checked="" type="checkbox"/>	<input type="checkbox"/> Flow cytometry
<input checked="" type="checkbox"/>	<input type="checkbox"/> Magnetic resonance imaging